

# Simulation-Based Inference with Approximately Correct Parameters via Maximum Entropy

Rainier Barrett,<sup>1</sup> Mehrad Ansari,<sup>1</sup> Gourab Ghoshal,<sup>2</sup> and <sup>\*</sup>Andrew White<sup>1</sup>

<sup>1</sup>*Department of Chemical Engineering,  
University of Rochester, Rochester, NY 14627*

<sup>2</sup>*Department of Physics and Astronomy,  
University of Rochester, Rochester, NY 14627*

## Abstract

Inferring the input parameters of simulators from observations is a crucial challenge with applications from epidemiology to molecular dynamics. Here we show a simple approach in the regime of sparse data and approximately correct models, which is common when trying to use an existing model to infer latent variables with observed data. This approach is based on the principle of maximum entropy and provably makes the smallest change in the latent joint distribution to accommodate new data. This simple method requires no likelihood or simulator derivatives and its fit is insensitive to prior strength, removing the need to balance observed data fit with prior belief. We demonstrate this MaxEnt approach and compare with other likelihood-free inference methods across three systems; a linear simulator with Gaussian noise, a point particle moving in a gravitational field, and finally a compartmental mode of epidemic spread. We demonstrate that our method compares favorably, and in some cases exceeds the performance of other methods.

## INTRODUCTION

Simulation-based inference (SBI) is a class of methods that infer the input parameters and unobservable latent variables in a simulator from observational data. SBI is different than traditional statistical inference or machine learning because simulators are typically not differentiable and their likelihoods are intractable. There have been great strides in methods for SBI and a recent review may be found in [1]. Most SBI methods are concerned with finding a few simulator parameters from a rich set of observations [2–4]. Here, we consider updating a simulator with many trusted parameters to match a sparse set of observations. The motivating example for this line of research is in molecular dynamics simulations of proteins. These simulations require thousands of parameters and the observed data is on the order of 10 data points. An approach that has emerged in molecular dynamics simulations is maximum entropy (MaxEnt) biasing [5–8]. MaxEnt biasing minimally modifies the simulator to match observations. The premise of MaxEnt is that the original model is approximately correct and observations should be matched in expectation, which is not the usual approach in SBI. These two assumptions lead to a unique bias [9] to the simulator that is independent of the parameters and can be implemented as a simple reweighting procedure. The MaxEnt method’s run-time scales only with sample number, rather than the number of model parameters which is atypical of most SBI methods because they require joint sampling.

The result of this work is a method to reweight a black-box simulator to agree with observed data in a provably minimal way. The reweighted simulator can then be used to infer either better input parameters or other simulation outputs. The two conditions are that (i) the simulator is accurate enough that the observed data could have been derived from the simulator, either with noise or a prior belief distribution of the simulator’s input parameters; and (ii) predicted values for the observed data can be computed from the outcome of the simulator. The MaxEnt method result is an ensemble of outcomes from the simulator whose means agree with data and provide a regressed agreement to observed data while being as close to the original simulator outcomes as possible. The method is efficient, provides uncertainty estimates, and can account for unknown systematic errors.

The maximum entropy approach in simulation can be traced to Jayne’s early work on deriving statistical physics from MaxEnt [10]. It was shown, for example, that the Boltzmann

distribution could be derived by simply adding a restraint on average energy that must be satisfied in expectation, analogous to matching an observation. A similar method of incorporating observations in expectation returned 50 years later in determining how to match protein molecular dynamics simulations to observations [11]. This method was then recast as an approximation to MaxEnt [12] and matching observations in molecular dynamics to MaxEnt was shown in Pitera and Chodera [9]. This was followed by rapid progress to create practical methods for use in simulations [8, 13–15]. A recent review of these “minimal biasing” methods can be found in Bonomi et al [6]. The MaxEnt method based on reweighting, has been presented in the context of molecular dynamics simulations in many forms over the years [16–25].

Our contribution here is deriving a general MaxEnt framework that is applicable to arbitrary simulators, demonstrating its application to areas outside of molecular dynamics, and showing one method of improving the support (sampling) of the posterior, which is important when the simulator is far from the observations. In the remainder of this work, we develop the theory, discuss sampling issues, and compare the MaxEnt method to approximate Bayesian computing (ABC) [3, 26–28], Sequential neural likelihood (SNL) [29], and direct Bayesian inference when the likelihood is tractable.

## RESULTS

### Theory

Given a simulator  $f(\vec{\theta})$  with a set of parameters  $\vec{\theta}$ , we have a prior distribution of parameters  $P(\vec{\theta})$ . For example, the function  $f(\vec{\theta})$  could be propagating a system of ODEs for some set number of timesteps or a molecular dynamics simulation with intrinsic noise.

Suppose we have some set of  $N$  observations,  $\{\bar{g}\}_k$ ,  $k \in [1, \dots, N]$ , which we would like to match with our model. Assume the measurement of each  $\bar{g}_k$  has some uncertainty  $\epsilon_k$ , where  $\epsilon_k$  is a random variable distributed according to some prior distribution about uncertainty,  $P_0(\epsilon_k)$ . We would like to constrain our model such that

$$\int d\vec{\theta} d\epsilon P'(\vec{\theta}) g_k[f(\vec{\theta})] + \epsilon_k = E[g_k + \epsilon_k] = \bar{g}_k \forall k \quad (1)$$

This means that we want the average over the distribution of our updated models ( $P'(\vec{\theta})$ ) to match the observations data, with an allowable average disagreement based on  $\{\epsilon_k\}$ . This is an unusual constraint and is weaker than most simulation inference methods. It reflects the strong belief in our prior model in this setting. Note that  $P_0(\epsilon_k)$  is optional: it is not necessary to allow disagreement on average with data, unlike in a Bayesian framework. Another difference is that this distribution of uncertainty is about systematic bias. It accounts for systemic deviation in average agreement and does not describe the underlying variance of the observational data. This approach is analogous to Bayesian model averaging [30], in that it is an average over many model parameter settings, reweighted by the posterior likelihood.

The unique maximum entropy modification to the prior distribution  $P(\vec{\theta})$  to satisfy the  $N$  constraints is given by [8, 9, 12, 31]

$$P'(\vec{\theta}, \vec{\epsilon}) = \frac{1}{Z'} P(\vec{\theta}) \prod_k^N e^{-\lambda_k g_k[f(\vec{\theta})]} e^{-\lambda_k \epsilon_k} P_0(\epsilon_k), \quad (2)$$

$$Z' = \int d\vec{\theta} d\vec{\epsilon} P(\vec{\theta}) P_0(\epsilon) e^{-\sum_k \lambda_k (g[f(\vec{\theta})] + \epsilon_k)}, \quad (3)$$

where  $Z'$  is a normalization constant and  $\lambda_k$  are chosen such that  $E[g_k + \epsilon_k] = \bar{g}_k$ . The dependence on  $\vec{\epsilon}_k$  can be removed by computing the marginal,

$$P'(\vec{\theta}) = \int d\vec{\epsilon} P'(\vec{\theta}, \vec{\epsilon}) = \frac{1}{Z'} P(\vec{\theta}) \prod_k^N e^{-\lambda_k g_k[f(\vec{\theta})]} \int d\epsilon_k e^{-\lambda_k \epsilon_k} P_0(\epsilon_k). \quad (4)$$

The problem is reduced to finding  $\lambda_k$  such that the constraint is satisfied. Again, we must remove  $\vec{\epsilon}_k$  from  $E[g_k] + E[\epsilon_k] = \bar{g}_k$ , where  $E[\epsilon_k]$  is:

$$E[\epsilon_k] = \frac{\int d\epsilon_k e^{-\lambda_k \epsilon_k} P_0(\epsilon_k) \epsilon_k}{\int d\epsilon_k e^{-\lambda_k \epsilon_k} P_0(\epsilon_k)}, \quad (5)$$

and is understood to still be a function of  $\lambda_k$ . If we define  $\xi_k(\lambda_k) = E[\epsilon_k]$  the constraint equation can be rewritten as  $E[g_k] + \xi_k(\lambda_k) = \bar{g}_k$ .

---

**Algorithm 1:** MaxEnt Weights with Uncertain Observations

---

```

Input  $P(\vec{\theta})$ ,  $f(\vec{\theta})$ ,  $M$ , and  $N$  of  $P_0(\epsilon_k)$ ,  $g_k$ ,  $\bar{g}_k$ 
for  $i \leftarrow 1$  to  $M$  do
| Sample  $\vec{\theta}_i \sim P(\vec{\theta})$ 
| Evaluate  $g_k[f(\vec{\theta}_i)]$  for each  $\vec{\theta}_i \in \{\vec{\theta}\}_i$ 
end
while  $\sum_i w_i g_k[f(\vec{\theta}_i)] / \sum_i w_i + \xi_k(\lambda_k) \neq \bar{g}_k$  do
| for  $i \leftarrow 1$  to  $N$  do
| |  $w_i \leftarrow \prod_k e^{-\lambda_k g_k[f(\vec{\theta}_i)]} \int d\epsilon_k e^{-\lambda_k \epsilon_k} P_0(\epsilon_k)$ 
| |  $\lambda_k \leftarrow \lambda_k - \frac{\partial}{\partial \lambda_k} \left( \sum_k \bar{g}_k - \left[ g[f(\vec{\theta}_k)] w_i / \sum_i w_i + \xi_k(\lambda_k) \right] \right)$ 
| end
end
return  $\vec{w}$ 

```

---

### Computing weighted properties and sampling efficiency

In Algorithm 1, we show the procedure for sampling from the MaxEnt distribution defined in Equation 4 via importance sampling [32]. The output of this algorithm,  $\{w_i\}$ , are the weights of trajectories  $\{f(\theta_i)\}$ , and any desired property  $g$  can be computed as  $\sum_i g[f(\vec{\theta}_i)] w_i / \sum_i w_i$ .

The challenge of using MaxEnt is sampling from  $P'(\vec{\theta})$ . Our assumption thus far is that our prior  $P(\vec{\theta})$  is approximately correct, so that samples from  $P(\vec{\theta})$  should be similar to  $P'(\vec{\theta})$ . In this ideal case, the algorithm is simply a matter of reweighting. One samples  $\vec{\theta}_i$ , computes  $f(\vec{\theta}_i)$ , compute weights proportional to  $w_i[P'] = \prod_k^N e^{-\lambda_k g_k[f(\vec{\theta}_i)]}$  consistent with the experimental data (Algorithm 1), and then any other property is reweighted with the same weights. In the non-ideal case (if for instance sampling is expensive, the space is high-dimensional, or the model is far from correct), there can be insufficient support to agree with the constraints. To treat insufficient support, we take a simple approach and use gradient descent to modify the sampling distribution  $P^j(\vec{\theta})$  to minimize the cross-entropy with  $P'(\vec{\theta})$ :

$$P^{j+1}(\vec{\theta}) = P^j(\vec{\theta}) - \eta \frac{\delta}{\delta P^j(\vec{\theta})} \sum_i w_i[P'] \ln P(\vec{\theta}_i), \quad (6)$$

where  $w_i[P']$  depends on  $P^j(\vec{\theta})$  via the expectation function and  $\frac{\delta}{\delta P^j(\vec{\theta})}$  indicates a

functional derivative. We refer to this approach as *variational*.

### System 1: Simple Simulation with Gaussian Noise

As a first example of the applicability of our framework, we consider a simulator  $f$  that outputs a scalar  $r$ . We have a prior belief about the value of the constant as a normal distribution  $\mathcal{N}(\hat{r}, \theta)$ . This example serves to compare the MaxEnt approach with Bayesian inference. The observed data is a single point ( $r$ ) and we treat it as an average constraint in the MaxEnt. Figure 1 panel a) shows how the MaxEnt posterior changes with different observations ( $r = 5$  or  $r = 10$ ). The  $r = 10$  observation requires the variational sampling (Equation 6) because the observed value is outside the sampled support of the prior. The expected value of  $\hat{r}$  always matches the observation.

In the Bayesian inference method, we must provide some uncertainty with this point to create a probability distribution, namely  $P(\text{data}|\text{model})$  [33]. We take this to be  $\mathcal{N}(\hat{r}, \sigma)$ . Bayesian inference balances evidence with the prior distribution, and here that corresponds to the ratio of the prior variance ( $\theta^2$ ) with the variance of the noise in the observation ( $\sigma^2$ ). The expected value of  $\hat{r}$  will not match the observed value.  $E[\hat{r}]$  in the Bayesian setting will be between the observed value and the prior belief expectation. Figure 1 shows this two methods. Panel a) shows how the MaxEnt method leaves the variance of  $\hat{r}$  unchanged as we consider different observed values. Panel b) shows the use of Bayesian inference to match the observation at  $r = 10$ . It requires extreme ratios between prior belief and experimental uncertainty to match the observation at 10. Panel c) shows how the MaxEnt method keeps the distribution entropy maximized regardless of the observation value (x-axis), as expected for a maximum entropy method. Bayesian inference shows a more peaked distribution when the observed value is far away from the prior, giving less entropy. This is not a drawback, just the result of different assumptions.

### Example System 2: Point Particle Gravitation Simulation

For a second example, Figure 2 shows a comparison of SNL and MaxEnt reweighting on a unit mass particle in a gravitational field of three attractors. The simulator here is a

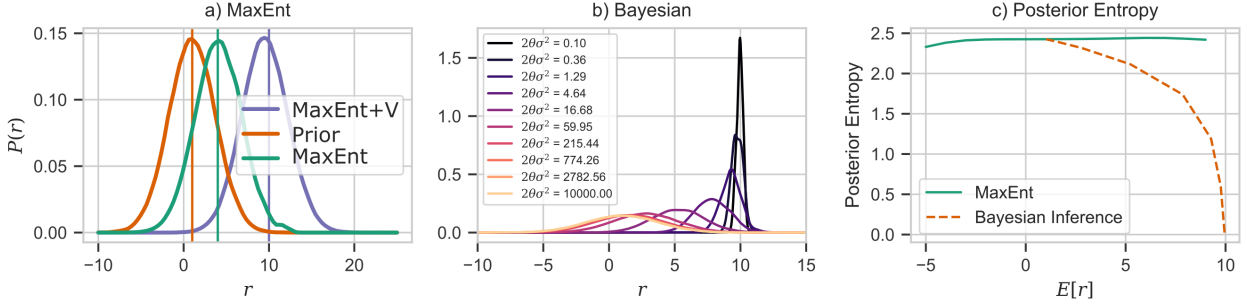


FIG. 1. **Comparison of Bayesian inference and MaxEnt reweighting.** Panel a) shows the simulator prior distribution in orange and the two versions of MaxEnt posterior with observations of 5 and 10. (MaxEnt+V stands for variational MaxEnt.) Panel b) shows the interplay between strength of prior and assigned uncertainty to the observation at 10 for Bayesian inference. Panel c) compares the posterior entropy of the two as a function of the observation location.

point particle following Newtonian gravitational mechanics. The goal here is to modify the simulation trajectories to align with a small set of observations. An example task might be fitting the trajectory of a comet to a small number of observations separated by years.

The parameters for this simulation were  $m_1$ ,  $m_2$ ,  $m_3$ ,  $v_{0x}$  and  $v_{0y}$ , the masses of the three attractors, and the initial velocity of the particle, respectively. The positions of the attractors and the initial position of the particle were all fixed. We treat these parameters as unknown, and the prior belief for them follows a normal distribution, shown in Figure 2. Repeatedly sampling from this prior and running the simulator results in a distribution of trajectories, whose means are shown in Figure 2a). MaxEnt reweights this ensemble of trajectories to agree with five observed positions along the trajectory. (The mean path does not exactly pass through the observations because some normally-distributed noise was imposed on each observation.) The average posterior trajectory indeed agrees with all observations. The prior and posterior for the parameters are shown in Figure 2b.

The observed points were generated from a “hidden” set of simulator parameters, i.e. the true parameters are not used as input to MaxEnt. Thus, one way to evaluate the MaxEnt performance is to see if the posterior means are close to these true values. We can see that the MaxEnt posteriors are closer to these values than the prior, but still largely in agreement with the prior. It fits the observations while staying as close to the prior as possible, because that maximizes entropy.

We computed the cross-entropy of the prior and posterior produced by MaxEnt and SNL.

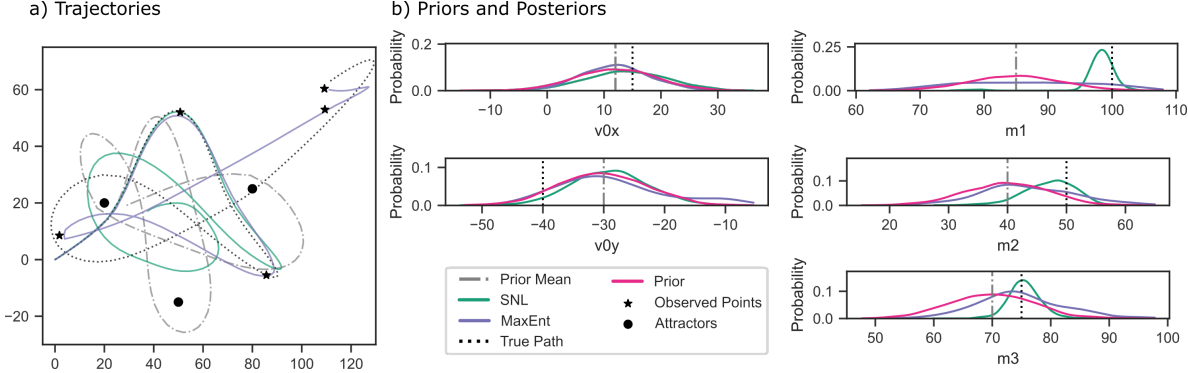


FIG. 2. **Comparison of SNL and MaxEnt methods on a gravitational field simulation of a particle moving through a fixed field with three attractors.** All units are SI values (m, m/s, kg). **a:** weighted mean paths generated by SBI with SNL (green) and MaxEnt (purple), alongside the path generated by the mean of the prior distribution (dash-dotted grey), and the true path used to generate observations (dashed black). Target points appear as black stars, and the attractors are black circles. **b:** Kernel density estimate of the posterior distribution of parameters after fitting, alongside their respective priors.

These values were 5.09 for SBI with SNL, and 3.43 for MaxEnt reweighting. This demonstrates how MaxEnt minimally alters the prior distribution while still matching observations in expectation – the average path followed by the MaxEnt particle matches all target points, while matching the posterior to the prior’s shape more closely than SNL.

### Example System 3: Epidemiological modeling

In our final example, we apply our framework to modeling the spread of a pathogen in vulnerable populations. We consider an SEAIR compartmental model of epidemic spread (Figure 3) on metapopulations connected via a spatial network of patches. Each patch corresponds to a location such as a zipcode in a city, or a county, and connections between patches correspond to mobility flows of residents encoded in a  $M \times M$  mobility matrix for  $M$  patches, where  $M_{ij}$  is the number of people moving from patch  $i$  to patch  $j$  in one time increment. Contacts within patches occur in a fully-mixed mean field manner where individuals can be in any one of five states of infection: Susceptible (**S**), Exposed (**E**), Asymptomatic (**A**), Infected (**I**), and Resolved (**R**). The choice for this particular combination of compartments was inspired by its relevance in modeling the evolution of the current SARS-CoV-2 pandemic [34, 35]. Each individual patch is represented with fractions

of **S, E, A, I, R**, rather than the count of individuals within each compartment.

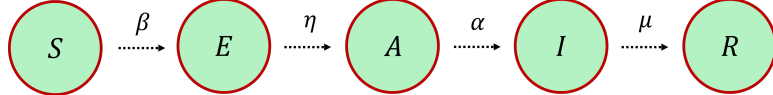


FIG. 3. **SEAIR model.** Populations in each patch can be in any one of Susceptible (**S**), Exposed (**E**), Asymptomatic (**A**), Infected (**I**) and Resolved (**R**). Susceptible individuals can get exposed to the disease by having contacts with the asymptomatic or the infected at infectivity rate  $\beta$ . Once exposed, they become asymptomatic and infected at rates  $\eta$  and  $\alpha$ . The infected finally recovers or dies at rate  $\mu$  and becomes resolved.

We first create a “reference” trajectory that represents the true disease model. From this reference trajectory, we extract observations which are used as the input to the MaxEnt methods, by extracting values at specific timepoints in the reference trajectory. A challenge in modeling the spread of epidemics is associated with reporting of the empirical number of confirmed cases (compartment **I**), which is typically very noisy [36]. To simulate this uncertainty, we add random additive noise to the observations from the reference trajectory (see Methods for details). This reference trajectory is represented as dashed lines in Figure 4a). We choose 5 uniformly random data points within the first half of the trajectory of the compartment **I** in patch 1 as observations (represented as black dots). The performance of the model is evaluated by comparing the predicted trajectory and the reference in a different patch (3). In Figure 4b) we compare the performance of MaxEnt, a least-squares fit, and ABC in fitting the prior to the observations. Compared to MaxEnt, the result from the least squares method was a poor fit with high variance, as it over-fits to observation noise. This was shown by doing a 5-fold leave-one-out cross-validation of the observations and evaluating the standard deviation at times  $t = 0, 125$  and  $250$  for each method (inset in Figure 4.b). Out of all methods evaluated, ABC had the least variance, but was computationally more expensive to run, whereas MaxEnt can include more model parameters without additional computational cost.

## DISCUSSION

We have presented MaxEnt reweighting as an SBI method for altering an approximately-correct simulator to agree with observations. This method can be used on arbitrary simulators with arbitrary numbers of parameters, requiring only sufficient sampling of the prior distri-

bution. The simulator need not have derivatives or tractable likelihoods. We demonstrated this by comparing with other SBI methods using three different simulators in different example contexts. The framework is particularly effective and robust when data is scarce or expensive (epidemic spreading being an archetypal example). MaxEnt provably changes the prior minimally to fit observations. While the method was initially developed for and particularly well-suited for molecular dynamics simulations—where experimental observations are much more costly and few in number compared to simulation—as demonstrated here, its applicability has potential for use in any setting of stochastic modeling where the derivative of the simulator’s output with respect to latent variables is unavailable or intractable.

The approach to sampling described here is an implementation of variational inference to sample from the posterior. One could instead use Monte Carlo sampling. This would have the advantage of not requiring derivatives, but since the derivatives here are closed-form it is not computationally inconvenient to use importance sampling. MaxEnt’s advantages over other widely used SBI methods, such as SNL, are that it is simple to implement, requires no hyperparameter choices like a neural network design, and can fit observations in expectation.

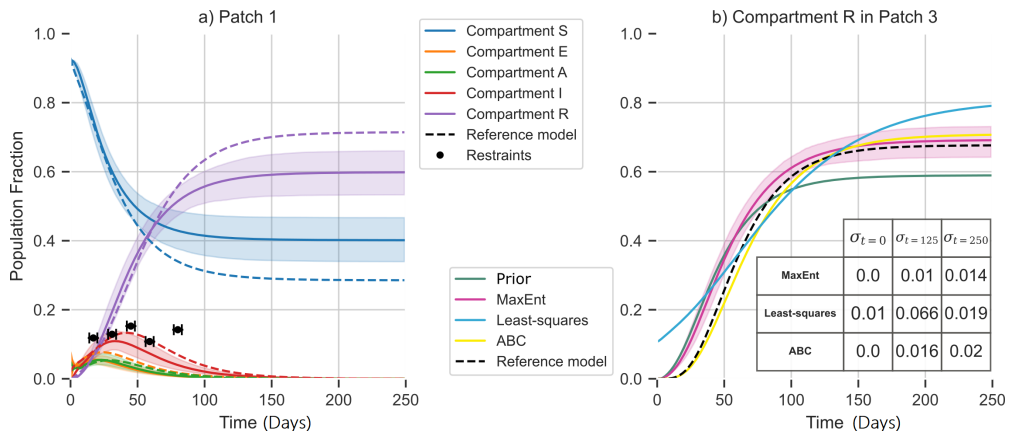


**FIG. 4. Maximum entropy reweighting of disease trajectory in a meta-population SEAIR model. a):** Prior-generated trajectory in one of the spatial patches for compartments S (blue), E (orange), A (green), I (red) and R (purple) are shown with solid lines and the reference trajectory is in dashed lines. The colored area represents the one-third higher and lower quantiles than average. Restraints (black circles) are selected random uniformly from compartment I with additive noise. **b):** Comparing the performance of MaxEnt (pink), Least-squares (blue), ABC (yellow) in fitting to reference model (black dashed line) in patch 3, based on observations in patch 1. Table inset shows standard deviations from 5-fold cross validation of the observations at three different times.

## METHODS

### Point Particle Gravitation Simulation

For this simulation, the prior parameter distribution was taken as a multivariate normal distribution centered at  $\{m_1 = 85, m_2 = 40, m_3 = 70, v_{0x} = 12, v_{0y} = -30\}$ , with covariance matrix  $\mathbf{I} \times 50$ . This wide prior was chosen because MaxEnt needs parameter support that overlaps with the observations we would like to fit. Fitting was done using the SBI package for Python [37] with the SNL method, [29] and a custom implementation of MaxEnt reweighting using Keras [38, 39]. Both methods used 2048 prior samples for fitting. SNL used default parameters from the SBI package [37] and MaxEnt used the Adam optimizer [40] with a learning rate of 0.0001 with mean squared error for 30000 epochs and batch size 2048.

### Epidemiology Modeling

Epidemic spreading in networks can be modeled as a reaction-diffusion process. The reaction corresponds to an infection caused by interactions of subjects within a fully-mixed region or patch of varying granularities (a meta-population), while diffusion corresponds to movement of people (of various infection states) between patches [41]. In this example, the meta-population system is comprised of three isolated local populations (patches) connected via flows corresponding to migrating individuals. The spreading process is represented through a temporally discretized ODE that includes the spatial distribution of the population as well as their mobility patterns [42].

In our simulation, the infection begins in patch 1, propagating to the other two patches according to a synthetic mobility matrix. This mobility matrix was randomly generated with dominating diagonal elements to satisfy the fully-mixed region assumption. Five uniformly random data points within the first half of the trajectory of the compartment **I** in patch 1 were considered as observations. Parameters for this simulation were asymptomatic, infectious and exposed periods along with the fractional starting values for **I** and **A** compartments. The prior parameter distribution were taken as a truncated-normal distribution centered at  $\{start_I = 0.001, start_A = 0.001, E_{period} = 2, A_{period} = 2, I_{period} = 10\}$ , with variances of

$\{0.8, 0.8, 1, 4, 5\}$ , respectively. For the simulation, the pyABC [43] package was used with default parameters, and the same MaxEnt implementation was used with the Adam optimizer, a learning rate of 0.01, and loss of mean squared error for 1000 epochs with a batch size of 8192. The SEAIR model implementation used in this work is publicly available as a python package at <https://github.com/ur-whitelab/maxent-epidemiology>.

## Acknowledgements

Funding for this research was provided by National Science Foundation under Grant No 2029095.

---

- [1] Kyle Cranmer, Johann Brehmer, and Gilles Louppe. The frontier of simulation-based inference. *Proceedings of the National Academy of Sciences*, page 201912789, may 2020.
- [2] Donald B Rubin. Bayesianly justifiable and relevant frequency calculations for the applies statistician. *The Annals of Statistics*, pages 1151–1172, 1984.
- [3] Mark A Beaumont, Wenyang Zhang, and David J Balding. Approximate bayesian computation in population genetics. *Genetics*, 162(4):2025–2035, 2002.
- [4] Peter J Diggle and Richard J Gratton. Monte carlo methods of inference for implicit statistical models. *Journal of the Royal Statistical Society: Series B (Methodological)*, 46(2):193–212, 1984.
- [5] Pietro Sormanni, Damiano Piovesan, Gabriella T Heller, Massimiliano Bonomi, Predrag Kukic, Carlo Camilloni, Monika Fuxreiter, Zsuzsanna Dosztanyi, Rohit V Pappu, M Madan Babu, Sonia Longhi, Peter Tompa, A Keith Dunker, Vladimir N Uversky, Silvio C E Tosatto, and Michele Vendruscolo. Simultaneous quantification of protein order and disorder. *Nat. Chem. Biol.*, 13(4):339–342, 2017.
- [6] Massimiliano Bonomi, Gabriella T Heller, Carlo Camilloni, and Michele Vendruscolo. Principles of protein structural ensemble determination. *Current opinion in structural biology*, 42:106–116, 2017.

- [7] Simon Olsson, Jes Frellsen, Wouter Boomsma, Kanti V Mardia, and Thomas. Hamelryck. Inference of structure ensembles of flexible biomolecules from sparse, averaged data. *PLoS One*, 8(11):e79439, 2013.
- [8] Dilnoza B Amirkulova and Andrew D White. Recent advances in maximum entropy biasing techniques for molecular dynamics. *Molecular Simulation*, 45(14-15):1285–1294, 2019.
- [9] Jed W Pitera and John D Chodera. On the Use of Experimental Observations to Bias Simulated Ensembles. *Journal of Chemical Theory and Computation*, 8(10):3445–3451, 2012.
- [10] Edwin T Jaynes. Information theory and statistical mechanics. *Physical review*, 106(4):620, 1957.
- [11] Shahidul M Islam, Richard A Stein, Hassane S Mchaourab, and Benoît Roux. Structural refinement from restrained-ensemble simulations based on epr/deer data: application to t4 lysozyme. *The journal of physical chemistry B*, 117(17):4740–4754, 2013.
- [12] Benoît Roux and Jonathan Weare. On the statistical equivalence of restrained-ensemble simulations with the maximum entropy method. *The Journal of chemical physics*, 138(8):02B616, 2013.
- [13] Andrea Cavalli, Carlo Camilloni, and Michele Vendruscolo. Molecular dynamics simulations with replica-averaged structural restraints generate structural ensembles according to the maximum entropy principle. *The Journal of chemical physics*, 138(9):03B603, 2013.
- [14] Wouter Boomsma, Jesper Ferkinghoff-Borg, and Kresten Lindorff-Larsen. Combining experiments and simulations using the maximum entropy principle. *PLoS Comput Biol*, 10(2):e1003406, 2014.
- [15] Andrew D White and Gregory A Voth. Efficient and minimal method to bias molecular simulations with experimental data. *Journal of chemical theory and computation*, 10(8):3023–3030, 2014.
- [16] Sabine Reiſer, Silvia Zucchelli, Stefano Gustincich, and Giovanni Bussi. Conformational ensembles of an RNA hairpin using molecular dynamics and sparse NMR data. *Nucleic Acids Research*, 48(3):1164–1174, 12 2019.
- [17] Kyle A Beauchamp, Vijay S Pande, and Rhiju Das. Bayesian energy landscape tilting: towards concordant models of molecular ensembles. *Biophysical journal*, 106(6):1381–1390, 2014.
- [18] Bartosz Rózycki, Young C Kim, and Gerhard Hummer. Sxas ensemble refinement of escrt-iii chmp3 conformational transitions. *Structure*, 19(1):109–116, 2011.

- [19] Hoi Tik Alvin Leung, Olivier Bignucolo, Regula Aregger, Sonja A Dames, Adam Mazur, Simon Berneche, and Stephan Grzesiek. A rigorous and efficient method to reweight very large conformational ensembles using average experimental data and to determine their relative information content. *Journal of chemical theory and computation*, 12(1):383–394, 2016.
- [20] Wing-Yiu Choy and Julie D Forman-Kay. Calculation of ensembles of structures representing the unfolded state of an sh3 domain. *Journal of molecular biology*, 308(5):1011–1032, 2001.
- [21] Pau Bernadó, Efstratios Mylonas, Maxim V Petoukhov, Martin Blackledge, and Dmitri I Svergun. Structural characterization of flexible proteins using small-angle x-ray scattering. *Journal of the American Chemical Society*, 129(17):5656–5664, 2007.
- [22] Konstantin Berlin, Carlos A Castaneda, Dina Schneidman-Duhovny, Andrej Sali, Alfredo Nava-Tudela, and David Fushman. Recovering a representative conformational ensemble from underdetermined macromolecular structural data. *Journal of the American Chemical Society*, 135(44):16595–16609, 2013.
- [23] Ivano Bertini, Andrea Giachetti, Claudio Luchinat, Giacomo Parigi, Maxim V Petoukhov, Roberta Pierattelli, Enrico Ravera, and Dmitri I Svergun. Conformational space of flexible biological macromolecules from average data. *Journal of the American Chemical Society*, 132(38):13553–13558, 2010.
- [24] Martin Pelikan, Greg L Hura, and Michal Hammel. Structure and flexibility within proteins as identified through small angle x-ray scattering. *General physiology and biophysics*, 28(2):174, 2009.
- [25] David E Shaw, Paul Maragakis, Kresten Lindorff-Larsen, Stefano Piana, Ron O Dror, Michael P Eastwood, Joseph A Bank, John M Jumper, John K Salmon, Yibing Shan, et al. Atomic-level characterization of the structural dynamics of proteins. *Science*, 330(6002):341–346, 2010.
- [26] Michael G B Blum and Chi Tran. HIV with contact tracing: a case study in approximate Bayesian computation. *Biostatistics*, 11(4):644–660, 2010.
- [27] Tina Toni, David Welch, Natalja Strelkowa, Andreas Ipsen, and Michael P.H Stumpf. Approximate Bayesian computation scheme for parameter inference and model selection in dynamical systems. *Journal of The Royal Society Interface*, 6(31):187–202, 2009.
- [28] Theodore Kypraios, Peter Neal, and Dennis Prangle. A tutorial introduction to Bayesian inference for stochastic epidemic models using Approximate Bayesian Computation. *Mathematical Biosciences*, 287:42–53, 2017.

- [29] George Papamakarios, David C. Sterratt, and Iain Murray. Sequential neural likelihood: Fast likelihood-free inference with autoregressive flows. *ArXiv*, 2019.
- [30] Andrew Gordon and Wilson Pavel Izmailov. Bayesian Deep Learning and a Probabilistic Perspective of Generalization. *Arxiv*, 2020.
- [31] Andrea Cesari, Alejandro Gil-Ley, and Giovanni Bussi. Combining simulations and solution experiments as a paradigm for rna force field refinement. *Journal of chemical theory and computation*, 12(12):6192–6200, 2016.
- [32] Surya T. Tokdar and Robert E. Kass. Importance sampling: a review. *Wiley Interdisciplinary Reviews: Computational Statistics*, 2(1):54–60, jan 2010.
- [33] Gerhard Hummer and Jürgen Köfinger. Bayesian ensemble refinement by replica simulations and reweighting. *The Journal of chemical physics*, 143(24):12B634\_1, 2015.
- [34] Peng Zhou, Xing-Lou Yang, Xian-Guang Wang, Ben Hu, Lei Zhang, Wei Zhang, Hao-Rui Si, Yan Zhu, Bei Li, Chao-Lin Huang, et al. A pneumonia outbreak associated with a new coronavirus of probable bat origin. *nature*, 579(7798):270–273, 2020.
- [35] Fan Wu, Su Zhao, Bin Yu, Yan-Mei Chen, Wen Wang, Zhi-Gang Song, Yi Hu, Zhao-Wu Tao, Jun-Hua Tian, Yuan-Yuan Pei, et al. A new coronavirus associated with human respiratory disease in china. *Nature*, 579(7798):265–269, 2020.
- [36] Marc Lipsitch, David L. Swerdlow, and Lyn Finelli. Defining the Epidemiology of Covid-19 — Studies Needed. *New England Journal of Medicine*, 382(13):1194–1196, mar 2020.
- [37] Alvaro Tejero-Cantero, Jan Boelts, Michael Deistler, Jan-Matthis Lueckmann, Conor Durkan, Pedro J. Gonçalves, David S. Greenberg, and Jakob H. Macke. sbi: A toolkit for simulation-based inference. *Journal of Open Source Software*, 5(52):2505, 2020.
- [38] Martín Abadi, Ashish Agarwal, Paul Barham, Eugene Brevdo, Zhifeng Chen, Craig Citro, Greg S. Corrado, Andy Davis, Jeffrey Dean, Matthieu Devin, Sanjay Ghemawat, Ian Goodfellow, Andrew Harp, Geoffrey Irving, Michael Isard, Yangqing Jia, Rafal Jozefowicz, Lukasz Kaiser, Manjunath Kudlur, Josh Levenberg, Dandelion Mané, Rajat Monga, Sherry Moore, Derek Murray, Chris Olah, Mike Schuster, Jonathon Shlens, Benoit Steiner, Ilya Sutskever, Kunal Talwar, Paul Tucker, Vincent Vanhoucke, Vijay Vasudevan, Fernanda Viégas, Oriol Vinyals, Pete Warden, Martin Wattenberg, Martin Wicke, Yuan Yu, and Xiaoqiang Zheng. TensorFlow: Large-scale machine learning on heterogeneous systems, 2015. Software available from tensorflow.org.
- [39] François Chollet. keras. <https://github.com/fchollet/keras>, 2015.

- [40] Diederik P. Kingma and Jimmy Ba. Adam: A method for stochastic optimization. *CoRR*, abs/1412.6980, 2014.
- [41] Jesús Gómez-Gardenes, David Soriano-Panos, and Alex Arenas. Critical regimes driven by recurrent mobility patterns of reaction–diffusion processes in networks. *Nature Physics*, 14(4):391–395, 2018.
- [42] Alex Arenas, Wesley Cota, Jesus Gomez-Gardenes, Sergio Gómez, Clara Granell, Joan T Matamalas, David Soriano-Panos, and Benjamin Steinegger. A mathematical model for the spatiotemporal epidemic spreading of covid19. *MedRxiv*, 2020.
- [43] Emmanuel Klinger, Dennis Rickert, and Jan Hasenauer. pyABC: distributed, likelihood-free inference. *Bioinformatics*, 34(20):3591–3593, 05 2018.